COMPLETED

Photocatalytic Reduction of CO_2 to CO in the Presence of H_2 or CH_4 as a Reductant over MgO

Kentaro Teramura, Tsunehiro Tanaka,* Haruka Ishikawa, Yoshiumi Kohno, and Takuzo Funabiki

Department of Molecular Engineering, Graduate School of Engineering, Kyoto University, Kyoto 615-8510, Japan

Received: August 5, 2003; In Final Form: October 14, 2003

MgO exhibits activity for the reduction of CO_2 to CO under photoirradiation in the presence of H_2 or CH_4 as a reductant, although MgO is an insulating material. The present study clarified the mechanism of the CO_2 photocatalytic reduction in the presence of H_2 or CH_4 over MgO. The electron paramagnetic resonance (EPR) spectra show that a CO_2 molecule adsorbed on MgO was activated to a CO_2^- radical under photoirradiation. In addition, it was confirmed by photoluminescence that new acceptor level built up between the valence band and the conduction band of MgO on CO_2-adsorbed MgO. The CO_2^- radical was reduced to a surface bidentate formate or a surface bidentate acetate by H_2 or CH_4 in the dark, respectively. The surface bidentate formate anchors on MgO as a photoactive species and reduces CO_2 in the gas phase to CO since the CO_2 photocatalytic reduction proceeded over MgO absorbing HCHO or CH_3CHO and only ^{12}CO was formed in the presence of $^{12}CO_2$ over MgO modified by a ^{13}C-labeled formate under irradiation. The active species was generated from the side-on adsorption-type bidentate carbonate selectively, although the two types of bidentate carbonates were detected by Fourier transform infrared (FT-IR) spectroscopy. On the other hand, the role of the surface bidentate acetate is under discussion. It is the first report that the substrate-modified insulating material exhibits activity in the CO_2 photocatalytic reduction.

Introduction

Carbon dioxide is well-known as a greenhouse effect gas. However, it is common knowledge that CO_2 is a very stable and inert compound. CO_2 cannot be easily reduced under mild conditions of room temperature and atmospheric pressure. For example, a CO_2 reforming system is recognized widely as a method to produce synthesis gas (i.e., $CO + H_2$), which can be used in chemical energy transformation systems or utilized in the Fischer−Tropsch reaction to produce liquid. The reaction formulas in the cases with H_2 or CH_4 as reductant are as follows:

$$CO_2 + H_2 = CO + H_2O \quad \Delta H° = 9.8 \text{ kcal/mol} \qquad (1)$$

$$CO_2 + CH_4 = 2CO + 2H_2 \quad \Delta H° = 59.1 \text{ kcal/mol} \qquad (2)$$

It is well-known that these reactions are achieved at 1000 K and in 2−4 MPa over Ni catalyst. In addition, methanation between CO_2 and H_2 ($CO_2 + 4H_2 = CH_4 + 2H_2O$), which is an important industrial process, is also carried out under high temperature and pressure. Therefore, development of a CO_2 reduction system that can proceed under mild condition is absolutely required.

Recently, the application of photocatalysts has received much attention since the photocatalytic reactions can be operated under mild conditions. Photocatalytic reduction of CO_2 is also one of the most attractive reactions in addition to photocatalytic decomposition of H_2O and photocatalytic reduction of N_2 to NH_3 because high temperature and pressure are necessary for the transformation of CO_2. In particular, from the viewpoint of natural green plant photosynthesis, there are many reports about the photocatalytic reduction of CO_2 in the presence of H_2O as a reductant over various semiconductor photocatalysts. Inoue et al.[1] have first reported that CO_2 bubbled in water is reduced to HCHO, HCOOH, and CH_3OH over various semiconductor photocatalysts such as TiO_2, ZnO, CdS, GaP, and SiC under photoirradiation of the aqueous suspension. Above all, SiC semiconductor photocatalyst exhibited the highest activity in the suspension photocatalysis system. Contemporaneously, Hemminger et al.[2] investigated the photosynthetic reaction of CO_2 and H_2O in the gas phase to form CH_4 over Pt−$SrTiO_3$. On the other hand, Fruge et al.[3] described the formation of organic molecules from $CO_2 + H_2O$ over Pt that included chlorophyll under visible light irradiation. These reports on the CO_2 photocatalytic reduction with H_2O having appeared from 1978 through 1980 stimulated many research groups, resulting in the active production of many following reports. The semiconductor materials applied to this reaction brought about various topics. The reported products were HCHO, HCOOH, CH_3OH, C_2H_5OH, CH_3CHO, CH_4, and C_2H_6. Halmann and coworkers[4−7] published many papers on the CO_2 photocatalytic reduction over various semiconductor materials, inspired by their photoelectrochemical results. Tennakone[8] carried out screening of the CO_2 photocatalytic reduction over various metal−supported titanium oxides (Pt, Au, Ag, Co, Pb, and Hg) and demonstrated that Hg-coated TiO_2 shows the highest activity to obtain HCHO. Tennakone et al.[9] also examined the CO_2 photocatalytic reduction with hydrous cuprous oxide ($Cu_2O\cdot xH_2O$). In the case of the suspension system, CO_2 dissolves in water and is transformed into CO_3^- or HCO_3^-. Photocatalytic reduction of carbonate and bicarbonate had been carried out in order to investigate the reaction mechanism since Chandraseka-

* Corresponding author: e-mail tanaka@dcc.mbox.media.kyoto-u.ac.jp; fax +81-75-383-2561.

10.1021/jp0362943 CCC: $27.50
Published on Web 12/10/2003

ran et al.[10] reported the photocatalytic reduction of carbonate to formaldehyde on TiO_2 powder.

On the other hand, some groups have reported the photocatalytic reduction of CO_2 with H_2O in the gas phase. Anpo and co-workers[11−15] described that highly dispersed titanium oxide on SiO_2, Vycor glass, Y-zeolite, and β-zeolite indicates activity to produce CH_4 and CH_3OH for the photoreduction of CO_2 in the presence of H_2O in the gas phase. The evolution rates of CH_4 and CH_3OH in all their reports were several nanomoles per gram of catalyst per hour or micromoles per gram of Ti per hour. The activity would be very low. In addition, they investigated that TiO_2(100) has a higher activity than TiO_2-(110) for the CO_2 photoreduction with H_2O in the gas phase.[16] Saladin et al.[17,18] reported the photosynthesis of CH_4 over irradiated TiO_2 from gaseous H_2O and CO_2. The formation of O_2 for the photoreduction of CO_2 with H_2O was first investigated by Ogura et al.[19] The maximum yield of H_2 was exhibited with highly dispersed 0.5 wt % CeO_2-TiO_2.

There are seldom reports of the CO_2 photocatalytic reduction in the presence of reductant except H_2O. Thampi et al.[20] have already investigated the methanation of CO_2 with H_2 under mild conditions with Ru/TiO_2 catalyst, which was developed by Kohno et al.,[21,22] who used Rh/TiO_2 catalyst. The photocatalytic reduction of CO_2 in the presence of H_2S as a reductant was reported by Aliwi and Aljubori.[23] We also reported that the reduction of CO_2 takes place in the presence of H_2 or CH_4 as a reactant over irradiated ZrO_2, and then CO and H_2 were formed in the gas phase.[24−28] The mechanism for the photocatalytic reduction of CO_2 over ZrO_2 cannot be explained by a simple band theory although ZrO_2 is also a semiconductor. According to phosphorescence excitation spectra, the emission intensity increased at above 300 nm after introduction of CO_2 although the maximum emission intensity of ZrO_2 was obtained at 270 nm.[26] It was confirmed that the band-gap excitation of zirconium oxide is unnecessary for the photocatalytic reduction of CO_2. We proposed the mechanism of the CO_2 photocatalytic reduction in the presence of H_2 or CH_4 over ZrO_2 as follows. CO_2 adsorbed on the surface of ZrO_2 is photoexcited under photoirradiation to the CO_2^- anion radical. The CO_2^- radical reacts with H_2 to form the surface formate. In the presence of CH_4 as a reactant, the surface acetate as well as the surface formate is generated. The surface acetate cannot react further but remains on the surfaces. The surface formate acts as a reactant of another CO_2 to CO under photoirradiation. During the reduction of CO_2 by the surface formate, the formate itself is oxidized to the adsorbed CO_2 species again. The production of CO proceeds via the two-step reaction. This suggests that the reaction can be catalyzed by materials that are not semiconductors.

In searching for many reports relevant to the CO_2 photocatalytic reduction, we found that titanium oxide and metal-loaded titanium oxide have been usually used as photocatalysts. It is noted that titanium oxide is a semiconductor photocatalyst and metals are often loaded in order to promote the charge separation. It is thought that semiconductors are well suited to photocatalysts because the photocatalytic system is based on the excitation of electrons from the valence band to the conduction band. We have reported the photocatalytic reduction of CO_2 in the presence of H_2 as a reductant over MgO.[29] It was confirmed that the photocatalytic reduction of CO_2 proceeds over MgO although MgO is an insulating material. CO and H_2 were produced in this reaction. Therefore, the mechanism of the CO_2 photocatalytic reduction cannot be explained by the simple band-gap irradiation. In the present study, we carried out the photocatalytic reduction of CO_2 over MgO in the presence of CH_4 as well as H_2. In addition, the photoactivated species on MgO was identified by electron paramagnetic resonance spectroscopy (EPR) and luminescence.

Experimental Section

Materials. The magnesium oxide supplied from the Merck was hydrated in distilled water for 2 h at 353 K and filtered with a pump. After that, the sample was kept at 383 K for 24 h in an oven, followed by calcinations in air at 873 K for 3 h. The sample was ground to a powder under 100 mesh after calcination. The specific surface area is evaluated to be 110 m^2 g^{-1} by the BET method using N_2 adsorption isotherm at 77 K.

Estimation of Amount of Chemisorbed CO_2. Amount of chemisorbed CO_2 on MgO was determined by the adsorption equilibrium method as follows. MgO (0.3 g) was evacuated at 673 K as a beforehand treatment. CO_2 was introduced to MgO and an adsorption isotherm was measured at room temperature. Subsequently, CO_2 was evacuated through a N_2 liquid trap for 30 min at room temperature. After that, CO_2 was introduced to MgO and the adsorption isotherm was measured again. We subtracted the second adsorbed amount from the first one at the same equilibrium pressure to account for the physisorbed CO_2. The value obtained by the subtraction represents the amount of chemisorbed CO_2.

Reactions. Reactants were purified prior to use for reactions in the following manner. Hydrogen was purified by passing it through a liquefied nitrogen trap. Carbon dioxide, methane, and acetaldehyde were purified by vacuum distillation at the temperature of liquid nitrogen. ^{13}C-Labeled carbon dioxide and methane were commercially supplied from Icon and used without further purification. Formaldehyde was obtained by heating paraformaldehyde in a vacuum. Acetaldehyde was purified by vacuum distillation with a liquefied nitrogen trap.

The reaction was carried out in a closed static system connected to a vacuum line. A 0.3 g amount of magnesium oxide was spread on the flat bottom of a quartz reactor (dead space 18.9 mL). Prior to photocatalytic reduction, the catalyst sample was heated at 673 K in air and evacuated for 30 min at the same temperature, followed by treatment with 8 kPa of O_2 for 90 min and evacuation for 30 min at 673 K. The mixture of substrate (CO_2, 150 μmol) and reductant (H_2 or CH_4, 50 μmol) was admitted into the reactor. The catalyst sample was irradiated from the flat bottom of the reactor through a reflection by a cold mirror with a 500 W ultra-high-pressure mercury lamp USH-500D supplied by Ushio Co. The area subjected to illumination was 12.6 cm^2. After each reaction, the gaseous products were analyzed, and after 5 min of evacuation at room temperature the sample was heated at 673 K for 30 min and the desorbed gases were also analyzed. The analysis of the products was performed with an on-line TCD gas chromatograph (Shimadzu GC-8A) equipped with a column packed with molecular sieve 5A and with Ar as a carrier gas. When formaldehyde or acetaldehyde was used as a reaction substrate, 5 μmol of the substrate was introduced onto 0.3 g of MgO with 150 μmol of CO_2 or 50 μmol of H_2 or CH_4 in the reactor.

Fourier Transform Infrared Spectroscopy. Infrared spectra of a sample and adsorbed species were recorded with a Perkin-Elmer Specrum One Fourier transform infrared spectrometer in a transmission mode at room temperature. A magnesium oxide sample (ca. 50 mg) was pressed into a wafer (diameter = 10 mm) at a pressure of 2.0 MPa and introduced in a conventional in situ IR cell equipped with NaCl windows. The cell allowed us to perform heating, O_2 treatment, introduction of substrates, photoirradiation, and measurements of spectra in

situ. Before a measurement, the sample was evacuated at 673 K for 30 min, followed by treatment with 8 kPa of O_2 for 90 min and evacuation for 30 min at 673 K. A 250 W ultra-high-pressure mercury lamp USH-250D supplied by Ushio Co. was used as a light source for photoirradiation of the wafer. For each spectrum, the data from 10 scans were accumulated at a resolution of 4 cm^{-1}.

Photoluminescence. Photoluminescence spectra were recorded at room temperature with a Hitachi F-3010 fluorescence spectrometer equipped with a phosphoresence unit, which enables us to record 1 ms delayed spectra, and an in situ cell. Before a measurement, the sample was pretreated under the same conditions as for FT-IR spectroscopy measurements. The effect of CO_2 adsorption on the photoluminescence was investigated by recording the spectra under the equilibrium adsorption of CO_2 at room temperature.

Electron Paramagnetic Resonance. Electron paramagnetic resonance (EPR) spectra were recorded with an in situ quartz cell on an X-band EPR spectrometer (JEOL JES-SRE2X) with 100 k Hz field modulation. Before a measurement, the sample was pretreated under the same condition as that of the IR spectra. The *g* values and the amount of radical species were determined by use of a Mn marker and TEMPOL (2,2,6,6-tetramethylpiperidine-1-oxyl), respectively. The effect of CO_2 adsorption onto MgO on the EPR spectra was investigated by recording the spectra after the equilibrium adsorption of CO_2 at room temperature followed by evacuation. Some spectra were recorded under illumination from a 500 W ultra-high-pressure mercury lamp USH-500D supplied by Ushio Co. Particular attention was paid to the removal of oxygen contamination to prevent the interference of the superoxide anion with the spectra. Prior to introduction into the cell, methane was passed through a Pt catalyst bed maintained at 473 K and then through a liquid nitrogen trap. CO_2 was purified by a freeze−pump−thaw process with a liquid nitrogen trap for several cycles.

Results and Discussion

Reactions. The products were CO and H_2 in the photocatalytic reduction of CO_2 with CH_4. CO (3.6 μmol) and H_2 (0.05 μmol) were formed over MgO in the presence of CO_2 and CH_4 under photoirradiation for 5 h at room temperature. In a previous study, we reported the photocatalytic reduction of CO_2 in the presence of H_2 as a reductant.[29] In this case, the CO evolution exhibited 2.9 μmol after 6 h of photoirradiation. It was found that CH_4 as well as H_2 operates as a reductant for the photocatalytic reduction of CO_2 over MgO. In addition, we have investigated the photocatalytic reduction of CO_2 over ZrO_2.[25,28] The CO evolution over MgO was 5 times higher than that over ZrO_2. When the reaction was carried out in the dark, without a catalyst or without a reactant (H_2 or CH_4), no CO or H_2 was detected in the gas phase. Figure 1 shows the time dependence of the amount of CO evolution and CH_4 consumption over MgO under photoirradiation. The rate of the CO evolution decreased gradually and was stopping after 30 h of photoirradiation. The evolution of CO and H_2 was 13.5 and 0.68 μmol after 30 h, respectively. The conversion of CO_2 was 9.0%. CH_4 was consumed exponentially until 12 h and the rate of the CH_4 consumption was constant after that. The amount of consumed CH_4 was considerably larger than that of evolved CO. The CH_4 consumption was not compatible with the CO evolution stoichiometrically. This suggests that intermediates anchor on the surface of MgO during the photocatalytic reduction of CO_2. We have confirmed that CO_2 was adsorbed on MgO readily. The origin of the carbon atom contained in the products and

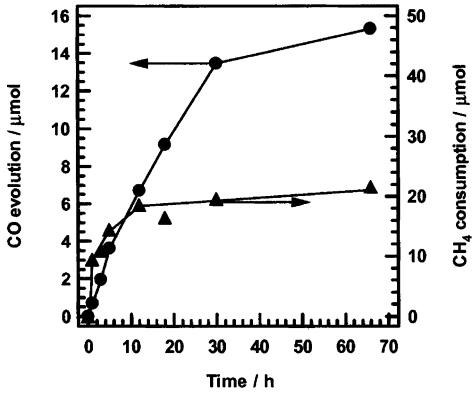

Figure 1. Time dependence of the amount of CO evolution (●) and CH_4 consumption (▲) over MgO under photoirradiation.

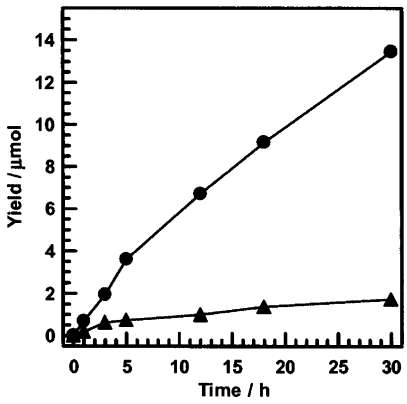

Figure 2. Time course of the CO products by the photocatalytic reaction (●) and by the heat treatment after photoirradiation (▲).

the surface species was determined by use of carbon isotopes (^{13}C-labeled CO_2 or CH_4). The carbon atom of either CO_2 or CH_4 was labeled by ^{13}C and the photocatalytic reduction of CO_2 with CH_4 was carried out over MgO. ^{13}CO or ^{12}CO was formed in the gas phase in the case of the $^{13}CO_2 + {}^{12}CH_4$ reaction or the $^{12}CO_2 + {}^{13}CH_4$ reaction, respectively. Therefore, all CO generated in the gas phase is derived from CO_2, and CH_4 does not merely reduce CO_2 to two CO molecules on the basis of the formula (eq 2). In the present reaction, the role of CH_4 is the reduction of CO_2 adsorbed on MgO because only 20 μmol of CH_4 was consumed. It is speculated that CO_2 species reduced by CH_4 anchors as an intermediate on MgO.

CO and H_2 were detected in the gas phase by heating the catalyst sample at 673 K for 30 min after the reaction. It is expected that the intermediate consists of hydrogen, carbon, and oxygen. It has been determined that formate is generated as an intermediate for the $CO_2 + H_2$ photocatalytic reaction over MgO or ZrO_2, and the amount of CO collected by heating the catalyst is equal to that of the formate formed on the surface.[24,26,27] On the other hand, it was reported that acetate is generated expect the formate for the $CO_2 + CH_4$ photocatalytic reaction over ZrO_2.[28] Figure 2 shows the time course of CO evolution by the photocatalytic reaction and by the heat treatment after irradiation. The CO amount after the catalyst was heated was constant against the irradiation time after 5 h, although the CO amount after irradiation increased gradually. The behavior of CO evolution upon heating of the catalyst sample is similar to that of CH_4 consumption. This also indicates that the amount of the intermediates which can be formed on MgO is limited. Figure 3 shows the dependence of the amount of CO evolved by the photocatalytic reaction and by the heat treatment after photocatalytic reaction on the initial amount of introduced CO_2. There

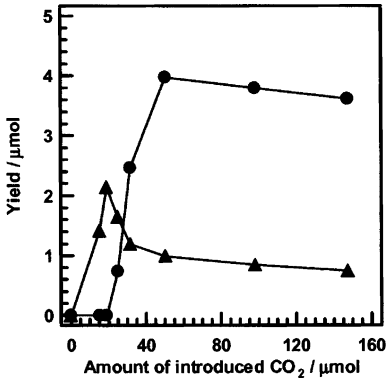

Figure 3. Dependence of the amount of CO evolved by the photocatalytic reaction (●) and by the heat treatment after photocatalytic reaction (▲) on the initial amount of introduced CO_2.

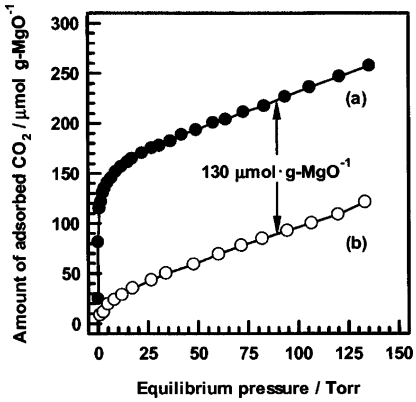

Figure 4. Adsorption isotherms of CO_2 on MgO (a) after pretreatment (●) and (b) after adsorption of CO_2 and evacuation (○).

was no CO evolution by the photocatalytic reaction until the amount of introduced CO_2 reached 20 μmol. The CO evolution increased gradually and was constant after CO_2 reached 40 μmol. On the other hand, CO evolution by the heat treatment after photocatalytic reaction was maximal when the amount of introduced CO_2 was 20 μmol. As mentioned previously, more than 20 μmol of CH_4 was not also consumed although light irradiation was elongated. Therefore, it is inferred that one CO_2 molecule was reduced by one CH_4 molecule to the intermediate species. The introduction of more than 40 μmol of CO_2 did not have a marked influence on the amount of either mode of CO evolution.

Estimation of Amount of Chemisorbed CO_2. In previous study, we have confirmed that about 40 μmol of CO_2 is chemisorbed on 0.3 g of MgO [133 μmol·g-MgO^{-1}].[29] The amount of chemisorbed CO_2 was determined as follows. CO_2 was trapped with a liquid N_2 after 150 μmol of CO_2 was introduced to MgO. The amount of trapped CO_2 was subtracted from that of introduced CO_2 which left the amount of chemisorbed CO_2. The amount of chemisorbed CO_2 [133 μmol·g-MgO^{-1}] was compatible with the minimum amount of introduced CO_2 in the maximum CO evolution by the photocatalytic reaction. In the present study, we obtained the adsorption isotherms of CO_2 on MgO as shown in Figure 4a. After that, CO_2 was adsorbed on MgO again as shown in Figure 4b. The subtraction between panels a and b was 130 μmol·g-MgO^{-1}. Thus, the amount of CO_2 chemisorbed on 0.3 g of MgO corresponds to 39 μmol. This value was almost compatible with that in previous study as mentioned above. Introduction of 66 μmol·g-MgO^{-1} of CO_2 caused the most CO evolution by the heat treatment. In addition, the CO evolution by the photocatalytic reaction could be detected in the gas phase after

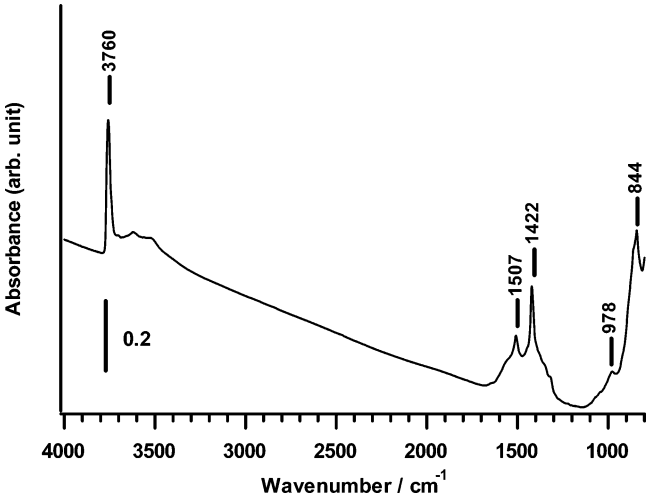

Figure 5. IR spectrum of MgO after pretreatment.

the amount of introduced CO_2 reached 66 μmol·g-MgO^{-1}. On the other hand, both CO evolutions by the photocatalytic reaction and by the heat treatment were constant after the amount of introduced CO_2 reached 133 μmol·g-MgO^{-1}. It is interesting that there are two different thresholds in the photocatalytic reduction of CO_2 over MgO. These results suggest that the species produced before the introduced CO_2 reached 66 μmol·g-MgO^{-1} is different from that produced after more than 66 μmol·g-MgO^{-1} of CO_2 was introduced.

Fourier Transform Infrared Spectroscopy. Figure 5 represents the IR spectra of MgO after pretreatment. A peak assigned to an OH stretching vibration band [ν(OH)] of a surface hydroxyl group is observed at 3760 cm^{-1}. In addition, five bands appeared at 1507, 1422, 978, 862 (shoulder), and 844 cm^{-1}. Raman[30,31] described the 985 and 845 cm^{-1} bands as overtones of fundamental frequencies at 490 and 425 cm^{-1}, respectively. Hanna[32] and Evans and Ehateley[33] agreed with these identifications. Accordingly, the bands at 978, 862, and 844 cm^{-1} in the present study are derived from an overtone of a fundamental lattice vibration (Mg−O stretching). It is known that the bands at 1400−1500 cm^{-1} are a C−O stretching vibration band [ν(C−O)] of carbonate ions.[33,34] Davydov et al.[35] reported that the bands at 1415 and 845 cm^{-1} are assigned to an asymmetric C−O stretching vibration band [ν_{as}(C−O)] and a deformation vibration band [$\delta(CO_3^{2-})$] of carbonate ion on MgO. The bands at 1507, 1422, and 844 cm^{-1} were assigned to carbonate ions. This carbonate ion would be derived from $MgCO_3$.[33] Considering this, the band at 844 cm^{-1} would be formed by overlapping the overtone of a fundamental lattice vibration and a deformation vibration of carbonate ion. Even evacuation at 673 K cannot remove $MgCO_3$ completely, since the decomposition temperature of $MgCO_3$ is higher than 673 K. CO_2 remaining as $MgCO_3$ after pretreatment is not involved in the reaction because CO was not generated under photoirradiation without the introduction of CO_2.

Figures 6 and 7 illustrate the difference IR spectra of the adsorbed species on MgO (a) after introduction of 4.1 kPa of CO_2 and evacuation, (b) after introduction of 5.1 kPa of H_2 or 5.2 kPa of CH_4 and under photoirradiation for 18 h, and (c) after evacuation (H_2 and CH_4 were used as reductant in Figures 6 and 7, respectively). The spectrum of pretreated MgO was used as a background of all difference IR spectra. When CO_2 was introduced to MgO, many bands appeared in the region of 1800−1250 cm^{-1} (Figures 6a and 7a). Davydov et al.[35] determined that the unidentate carbonate bands at 1520, 1320, and 1020−960 cm^{-1} are an asymmetric OCO stretching

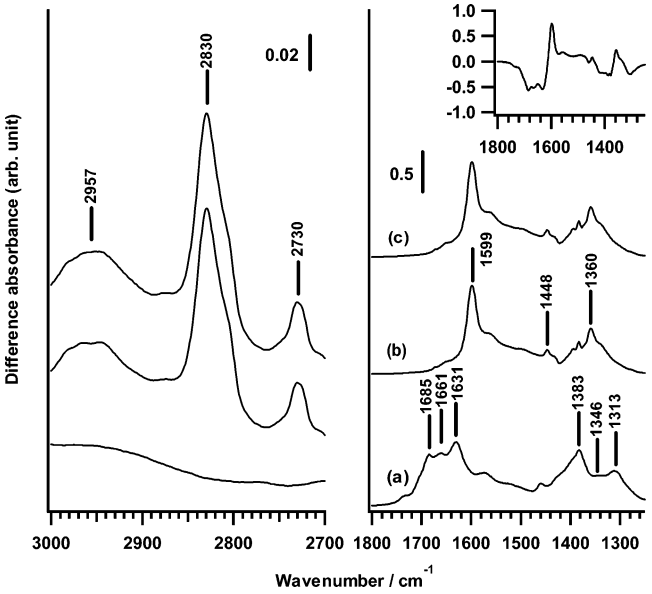

Figure 6. Difference IR spectra of the adsorbed species on MgO (a) after introduction of 3.9 kPa of CO_2 and evacuation, (b) after introduction of 5.1 kPa of H_2 and under photoirradiation for 18 h, and (c) after evacuation. The inset illustrates the difference spectrum between (a) and (b) in the region of 1800−1250 cm^{-1}, indicating the spectrum of adsorbate.

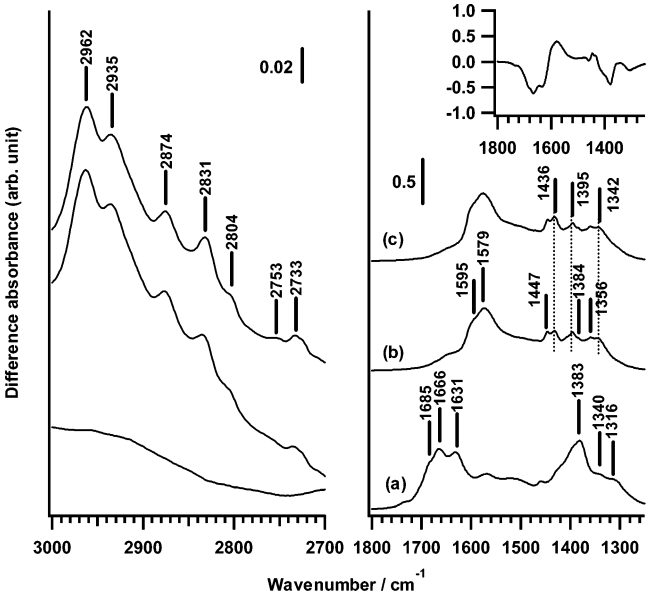

Figure 7. Difference IR spectra of the adsorbed species on MgO (a) after introduction of 3.9 kPa of CO_2 and evacuation, (b) after introduction of 5.2 kPa of CH_4 and under photoirradiation for 18 h, and (c) after evacuation. The inset illustrates the difference spectrum between (a) and (b) in the region of 1800−1250 cm^{-1}, indicating the spectrum of adsorbate.

vibration band [ν_{as}(OCO)], a symmetric OCO stretching vibration band [ν_s(OCO)], and a C−O stretching vibration band [ν(C−O)], respectively. In addition, they reported that the bicarbonate bands at 1700, 1455, and 1220 cm^{-1} are an asymmetric OCO stretching vibration band [ν_{as}(OCO)], a symmetric OCO stretching vibration band [ν_s(OCO)], and a C−O stretching vibration band [ν(C−O)], respectively.[35] In our case, the unidentate carbonate and the surface bicarbonate appeared at 1526 and 1337 cm^{-1} and at 1685 and 1383 cm^{-1}, respectively. On the other hand, bands at 1661, 1631, 1346, and 1313 cm^{-1} (1666, 1631, 1340, and 1316 cm^{-1} in Figure 7) are assigned to surface bidentate carbonates.[33,36−38] Fukuda and

CHART 1. Nature of Two Speculated Species[a]

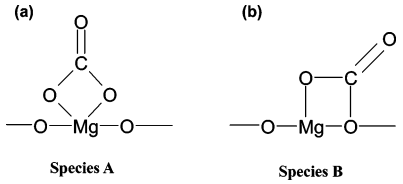

[a] Species A, one bidentate carbonate (stronger); species B, the other bidentate carbonate (weaker).

Tanabe[36] reported that two type of bidentate carbonate are generated at room temperature. In addition, Tsuji et al.[37] and Yanagisawa et al.[38] confirmed that the bands at 1668, 1320, 1005, and 849 cm^{-1} (species A as shown in Chart 1a) increase in intensity at 373 K by FT-IR spectroscopy and temperature-programmed desorption (TPD) methods, although the bands at 1630, 1277, 955, and 833 cm^{-1} (species B as shown in Chart 1b) disappear. It was concluded that species A is adsorbed more strongly on MgO than species B. However, the assignment of these two bidentate carbonate is under discussion. In a previous study, we also monitored the behavior of the absorbance of two bidentate bands by FT-IR spectroscopy when introduced CO_2 was increased gradually. Both species were detected in introducing a small amount of CO_2.[29] The increase in the absorbance of the bidentate bands at 1660 and 1310 cm^{-1} (species A) stopped after introduction of CO_2 exceeded 66 μmol·g -MgO^{-1}. On the other hand, the bidentate band at 1624 cm^{-1} (species B) increased in absorbance when more than 66 μmol·g-MgO^{-1} of CO_2 was introduced. Therefore, in this study, it was also classified that the bands at 1661 and 1346 cm^{-1} are stronger than those at 1631 and 1313 cm^{-1}. As mentioned above, the maximum amount of the chemisorbed CO_2 was 130 μmol·g-MgO^{-1}. The most CO evolution by the heat treatment was achieved upon introducing 66 μmol·g-MgO^{-1} of CO_2. CO evolution by the photocatalytic reaction was confirmed in the gas phase when more than 66 μmol·gMgO^{-1} of CO_2 was introduced to MgO. And CO evolution by both the photocatalytic reaction and the heat treatment became constant after the amount of the introduced CO_2 reached 133 μmol·g-MgO^{-1}. The behavior obtained from the reaction is in agreement with that observed by IR spectra. In conclusion, the stronger bidentate carbonate (species A) is reduced to the mere intermediate, which is inactive for CO evolution. In introducing more than 66 μmol·g-MgO^{-1} of CO_2, the weaker bidentate carbonate (species B) is generated except species A. Species B is reduced to a surface-active intermediate that can produce CO in the gas phase from CO_2 by H_2 or CH_4 as a reductant because the amount of CH_4 consumption was compatible with that of species B evolution [66 μmol·g-MgO^{-1}].

Figures 6b and 7b show the IR spectra of MgO irradiated for 15 h in the presence of H_2 or CH_4 as a reactant after evacuation of CO_2. Increase or decrease in intensity and appearance of new bands were observed in the IR spectra in the region of 2900−2700 and 1800−1250 cm^{-1}. These spectra were not changed when MgO was left for 15 h in the presence of H_2 or CH_4 in the dark. The inset picture in Figure 6 shows the subtraction of the IR spectrum of adsorbed species on MgO in the presence of H_2 before photoirradiation (Figure 6a) from that after photoirradiation (Figure 6b). New bands at 2957, 2830, and 2730 cm^{-1} appeared in the region of 2900−2700 cm^{-1} under photoirradiation. These bands are assigned to a C−H stretching vibration band [ν(CH)].[39−42] Since surface carbonates have no C−H stretching vibration mode [ν(CH)], the appearance of these bands exhibits the formation of a surface species containing a C−H bond, which we expected to be a reaction

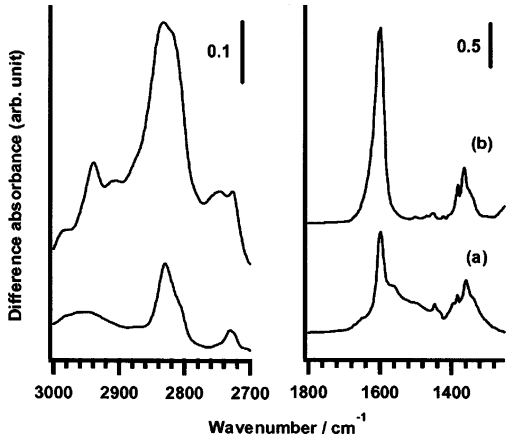

Figure 8. Difference IR spectra of the adsorbed species (a) on MgO after introduction of 5.1 kPa of H_2 and under photoirradiation for 18 h (same as Figure 6b) and (b) on pretreated MgO after introduction of formaldehyde.

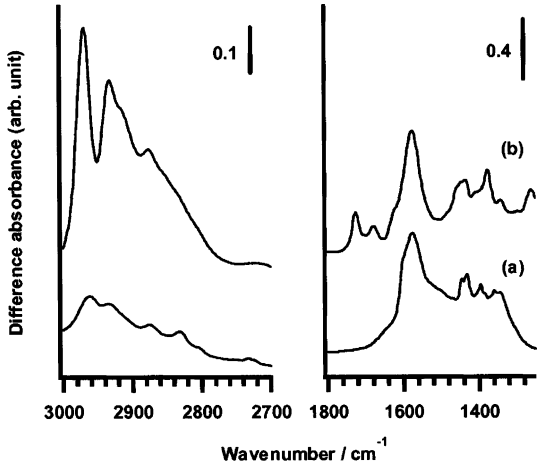

Figure 9. Difference IR spectra of the adsorbed species (a) on MgO after introduction of 5.2 kPa of CH_4 and under photoirradiation for 18 h (same as Figure 7b) and (b) on pretreated MgO after introduction of acetaldehyde.

intermediate.[29] In the region of 1800−1250 cm^{-1}, new bands at 1599 [ν_{as}(OCO)], 1448 [δ(CH)], and 1360 cm^{-1} [ν_s(OCO)] appeared under photoirradiation,[41−43] whereas the bands at 1668, 1634, and 1313 cm^{-1} assigned to a bidentate carbonate and the bands at 1686, 1459, and 1383 cm^{-1} assigned to a bicarbonate decreased in intensity. Accordingly, it is anticipated that the surface bidentate carbonate and the surface bicarbonate reacted with H_2 as a reductant under photoirradiation to the surface species containing a C−H bond. We have already confirmed that the new bands at 2957, 2830, 2730, 1599, and 1360 cm^{-1} were not formed in the dark or in the absence of H_2.[29] The new bands are derived from an intermediate species formed only in the presence of H_2 under photoirradiation because CO evolution by the heat treatment after the photoreaction is not observed without irradiation. In our previous papers,[26,27,29] we identified the intermediate for the $CO_2 + H_2$ reaction over ZrO_2 and MgO as a surface formate species; in addition, we found that a similar spectrum to that of the surface species was obtained when formic acid or formaldehyde was adsorbed on the surface of ZrO_2 or MgO, respectively. The difference IR spectrum of MgO irradiated for 15 h in the presence of H_2 after evacuation of CO_2 (same as Figure 6b) is similar to that of formaldehyde species adsorbed on pretreated MgO as shown in Figure 8. Wang and Hattori[44] reported that the bands at 2840 [ν(CH)], 1604 [ν_{as}(OCO)], and 1370 cm^{-1} [ν_s(OCO)] are assigned to a surface bidentate formate when formaldehyde is adsorbed on pretreated MgO. We have already proposed the molecular structure of the adsorbed species followed by Peng and Barteau.[45] Formaldehyde loses one hydrogen atom to connect with one lattice oxygen atom of MgO and forms a surface bidentate formate. Therefore, it was concluded that the surface species arising during the photoreaction between CO_2 and H_2 is a surface bidentate formate.

On the other hand, the inset picture in Figure 7 shows the subtraction of the IR spectrum of adsorbed species on MgO in the presence of CH_4 before photoirradiation (Figure 7a) from that after photoirradiation (Figure 7b). In the case of using CH_4 as a reductant, new bands in the region of 2900−2700 and 1800−1250 cm^{-1} were observed in addition to the bands in the case of using H_2 as a reductant; the bands at 1666, 1631, and 1316 cm^{-1} were assigned to a bidentate carbonate and the bands at 1684, 1460, and 1382 cm^{-1} were assigned to a bicarbonate decreased in intensity. In the range of 2900−2700 cm^{-1}, seven bands at 2962, 2935, 2874, 2831, 2804, 2753, and 2733 cm^{-1} were observed and assigned to ν_{as}(CH_3) (2962 cm^{-1}), ν_s(CH_3) (2935 cm^{-1}), and ν(CH) (2874, 2831, 2804, 2753, and 2733 cm^{-1}).[39−42] In the range of 1800−1250 cm^{-1}, new bands appeared at 1595 (s), 1579, 1447, 1436, 1395, 1384, 1356, and 1342 cm^{-1}. The bands at 1595, 1447, 1384, and 1356 cm^{-1} are assigned to ν_{as}(OCO), δ(CH), δ(CH), and ν_s(OCO), respectively, and derived from a formate because these bands were the same as that in the case of H_2 as a reductant.[41−43] In contrast, it was anticipated that the other bands were derived from an acetate. The band at 1579 cm^{-1} can be correlated to a C−O symmetric vibration mode.[46] The bands at 1436, 1395, and 1342 cm^{-1} are assigned to a C−H deformation vibration mode: δ_{as}(CH_3), δ(CH), and δ_s(CH_3), respectively.[47,48] As mentioned above, the spectrum of MgO irradiated in the presence of H_2 after evacuation of CO_2 was similar to that of pretreated MgO adsorbing formaldehyde (Figure 8). The surface species was a bidentate formate. Therefore, in the case of CH_4 as a reductant, it is expected that not only a bidentate formate but also a bidentate acetate are generated on MgO and the spectrum of MgO irradiated in the presence of CH_4 after CO_2 evacuation is similar to that of MgO adsorbing acetaldehyde. Khaleel et al.[49] reported that the adsorbed acetaldehyde interacts with lattice oxygen and transforms to a surface bidentate acetate when acetaldehyde is introduced to MgO. Figure 9 exhibits the difference IR spectra of acetaldehyde species adsorbed on pretreated MgO as compared with Figure 7b. The bands in the region of 3000−2700 cm and 1800−1250 cm^{-1} could be confirmed to be similar to those in Figure 7b. Consequently, the species adsorbed on MgO converts to the surface bidentate acetate as well as the surface bidentate formate as an intermediate in the presence of CH_4 under photoirradiation after CO_2 evacuation.

We carried out the CO_2 photocatalytic reduction over MgO pretreated with HCHO or CH_3CHO to investigate the role of the surface bidentate formate and the surface bidentate acetate as an intermediate. CO was not generated in the gas phase in the presence of only HCHO or CH_3CHO as a substrate under photoirradiation. In addition, we have no CO over MgO pretreated with HCHO or CH_3CHO in the presence of CH_4 as a reductant under photoirradiation. However, CO was detected in the gas phase when CO_2 was introduced to MgO in the presence of HCHO or CH_3CHO under photoirradiation. This reaction did not proceed in the dark. The origin of the carbon atom contained in the products and the surface species was determined by use of carbon isotopes (^{13}C-labeled CO_2). The

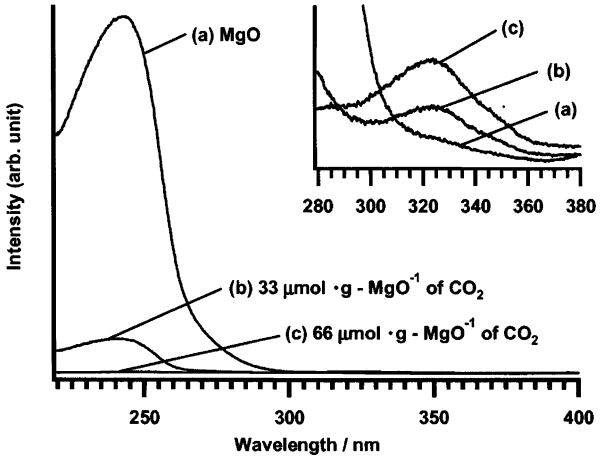

Figure 10. Phosphorescence excitation spectra of MgO (a) after pretreatment, (b) after introduction of 33 μmol·g-MgO^{-1} of CO_2 and (c) after introduction of 66 μmol·g-MgO^{-1} of CO_2.

carbon atom of CO_2 was labeled by ^{13}C and the photoreaction between $^{13}CO_2$ and $H^{12}CHO$ was carried out over MgO. Only ^{13}CO was formed in the gas phase. Therefore, CO generated in the gas phase is derived from CO_2.

These results are summarized as follows. Both the stronger bidentate carbonate (species A) and the weaker bidentate carbonate (species B) are generated when CO_2 is admitted to MgO. Species A increased by priority as compared with species B until the amount of introduced CO_2 reached 66 μmol·g-MgO^{-1}. In introducing more than 66 μmol·g-MgO^{-1} of CO_2, species B increased and CO was produced in the gas phase. The CO evolution by the photocatalytic reaction and the heat treatment became constant after more than 133 μmol·g-MgO^{-1} of CO_2 is introduced to MgO. This value is compatible with the amount of CO_2 chemisorbed on MgO [130 μmol·g-MgO^{-1}]. Therefore, the same amount of species A and species B [66 μmol·g-MgO^{-1}] are formed on MgO. In conclusion, species A would be connected with only magnesium atom and remain on MgO as an inactive species because there are excessive base sites of MgO. On the other hand, species B, which was adsorbed by the side-on adsorption-type form, is reduced to a surface bidentate formate or a surface bidentate acetate by H_2 or CH_4. These species are not intermediates but photoactive species on MgO because they are very stable and reduce CO_2 in the gas phase to CO.

Photoluminescence. From the FT-IR spectroscopy, it was investigated that the photoactive species for the CO_2 photocatalytic reduction is produced from a side-on adsorption-type carbonate (species B) and reduces CO_2 to CO. The adsorption of CO_2 on MgO is related to the mechanism of formate and acetate formations. The CO_2 species adsorbed on MgO is reduced to a surface bidentate formate or acetate in the presence of H_2 or CH_4 under photoirradiation, respectively. And the formate and the acetate contribute to the evolution of CO under photoirradiation. Therefore, it is anticipated that CO_2 adsorbed on MgO are photoactivated under photoirradiation. We have already reported the study of CO_2 adsorbed on ZrO_2 by UV−vis spectroscopy and photoluminescence.[26] In the case of ZrO_2, we have no spectral changes in the diffuse reflectance UV−vis spectra; however, there were some peaks caused by the formation of new photoactive species in photoluminescence. In this study, we also carried out to identify a photoactive species in photoluminescence. Figure 10 shows phosphorescent excitation spectra of MgO (a) after pretreatment, (b) absorbing 33 μmol·g-MgO^{-1} of CO_2 and (c) absorbing 66 μmol·g-MgO^{-1} of CO_2, and the inset is expanded at 280−380 nm. The emission light was monitored at 450 nm, because the maximum emission intensity was obtained at around that wavelength. The maximum excitation intensity, which was observed at 240 nm (5.2 eV), was assigned to excitation of bulk MgO. This result is reasonable as compared with the absorption band in the diffuse reflectance UV−vis spectrum, although Zecchina et al.[50] described that the absorption bands of lowest energy in undamaged crystal of MgO are at 61500 cm^{-1} (7.68 eV). On the other hand, Tench and Pott[51] reported the excitation intensity at 240 nm on MgO, in addition, Coluccia et al.[52−54] and Anpo et al.[55] investigated that the observed luminescence is derived from extrinsic lattice defects such as an F^+ center, an electron trapped at surface anion vacancy. In introducing CO_2 to MgO, the excitation intensity at 250 nm was quenched gradually. Therefore, CO_2 interacts with the extrinsic lattice defects. On the other hand, it is found that an absorption of the excitation wavelength at 320 nm increased in intensity when CO_2 was adsorbed on MgO. We obtained the same conclusion as ZrO_2. This shows that new bands build up between the valence band and conduction band of MgO. In addition, Figure 11 shows phosphorescent emission spectra excited at 320 nm of MgO (a) after CO_2 introduction and (b) after H_2 or CH_4 introduction to MgO-adsorbed CO_2. The broad peak observed at 350−600 nm was quenched after introduction of H_2 or CH_4. Thus, it is identified that the photoactive species derived from the adsorbed CO_2 interacts with H_2 or CH_4 as a reductant.

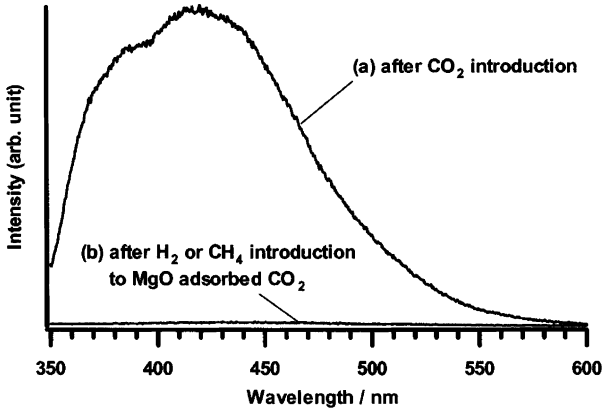

Figure 11. Phosphorescence emission spectra excited at 320 nm of MgO (a) after CO_2 introduction and (b) after H_2 or CH_4 introduction to MgO adsorbed CO_2.

Electron Paramagnetic Resonance. As mentioned above, we investigated whether the surface species derived from CO_2 adsorbed on MgO surface were photoactivated in a low energy. From many studies, the photoactivated CO_2 species on MgO was assigned to CO_2^- radical species.[38,56−58] Moreover, it was reported that CO_2 interacts with an F^+ center of MgO. We also measured EPR spectra to clarify the photoactivated CO_2 species in the present reaction. Figure 12 shows the EPR spectra of MgO with adsorbed CO_2 species. A signal derived from Mn^{2+} as an impurity appeared as shown in Figure 12a. This signal did not change although CO_2 was introduced to MgO in the dark. However, sharp signals (g = 1.998, 2.002 and g = 2.007, 2.011, 2.022) of two radical species were observed under photoirradiation. Only one signal (g = 2.001) was monitored when MgO was illuminated in the absence of CO_2. This signal was assigned to color center of MgO. Figure 13 represents the EPR spectra of MgO with adsorbed $^{13}CO_2$ species. Each signal was split into two when $^{13}CO_2$ was adsorbed instead of $^{12}CO_2$. Therefore, the signals in Figure 12c were not derived from MgO but the CO_2 species adsorbed on MgO. It was reported that g

SCHEME 1. Mechanism of Photocatalytic Reduction of CO_2 in the Presence of H_2 or CH_4

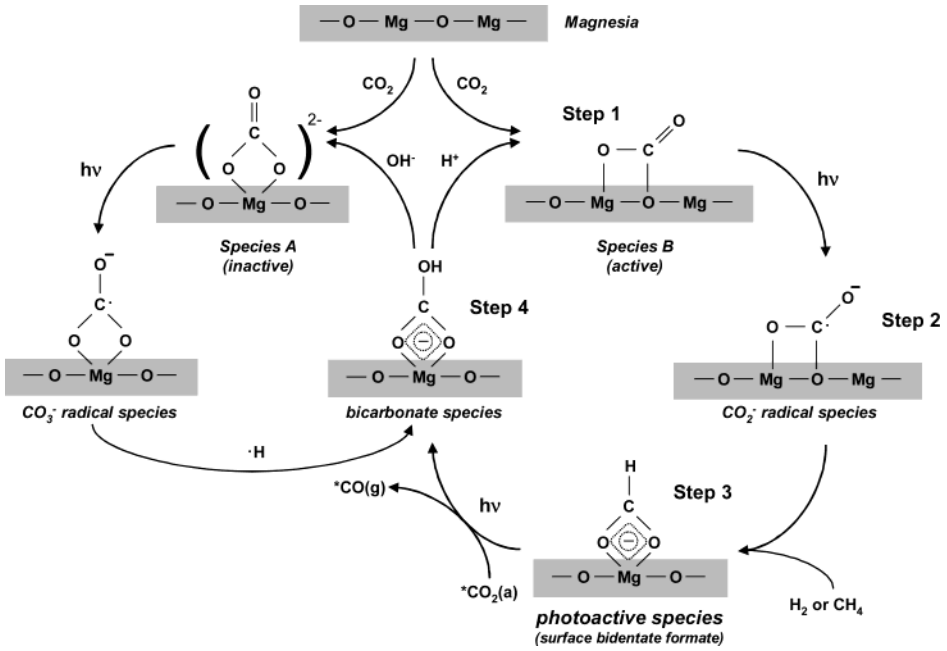

$= 1.998$, 2002 and $g = 2.007$, 2.011, 2.022 are assigned to a CO_2^- radical and a CO_3^- radical, respectively.[59−67] Our results are also supported by this assignment. In our case, the signals of the CO_2^- radical and the CO_3^- radical remained after 1 h although the light illumination was stopped. This indicates that the photoactivated species on MgO is very stable in the dark after photoirradiation. On the other hand, the CO_2^- radical and CO_3^- radical, the photoactivated species on MgO, react with H_2 or CH_4 as a reductant readily. When H_2 or CH_4 was introduced to MgO in the dark, the signals derived from the CO_2^- radical and CO_3^- radical disappeared in short order. In addition, the CO_2^- radical species vanished more quickly than the CO_3^- radical species. It is concluded that the CO_2^- radical is reduced by H_2 or CH_4 to the formate or the acetate rather than the CO_3^- radical in the present reaction.

Reaction Mechanism. From these results, we proposed the mechanism of the CO_2 photocatalytic reduction in the presence of H_2 or CH_4 as a reductant as shown in Scheme 1. The two bidentate carbonate are generated on MgO in introducing CO_2 as shown in Chart 1. Species A is the stronger bidentate carbonate than species B. The bidentate carbonates are activated under photoirradiation and are converted to a CO_2^- radical or a CO_3^- radical. The CO_3^- radical derived from species A would be transformed to the bicarbonate, which is inactive for the CO_2 photocatalytic reduction. On the other hand, the CO_2^- radical species derived from species B is reduced to a surface bidentate formate in the presence of H_2 or CH_4. The surface bidentate formate is very stable on MgO and reduced CO_2 in the gas phase to CO under photoirradiation. In the case of using CH_4 as a reductant, a surface bidentate acetate as well as a surface bidentate formate is generated on MgO. We speculate about the role of the acetate on MgO and suggest the following two possibilities: (1) a surface bidentate acetate is also an active species for CO_2 photocatalytic reduction, and (2) an inactive acetate is transformed to an active formate. In the case of the $CH_3CHO + CO_2$ reaction, the activity was lower than that of

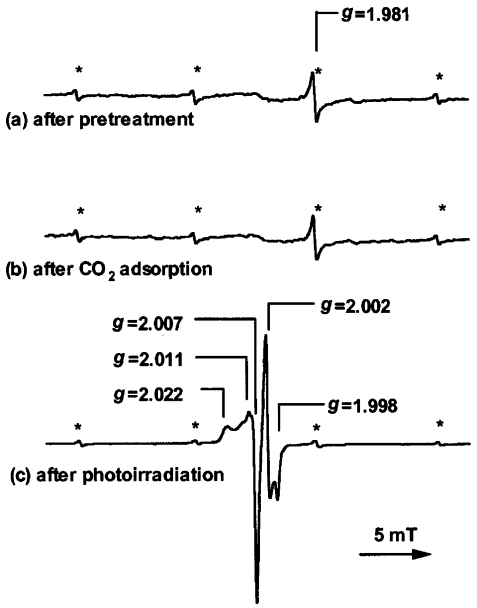

Figure 12. EPR spectra of MgO (a) after pretreatment, (b) after CO_2 adsorption, and (c) after photoirradiation. Asterisks indicate Mn^{2+} impurity in MgO.

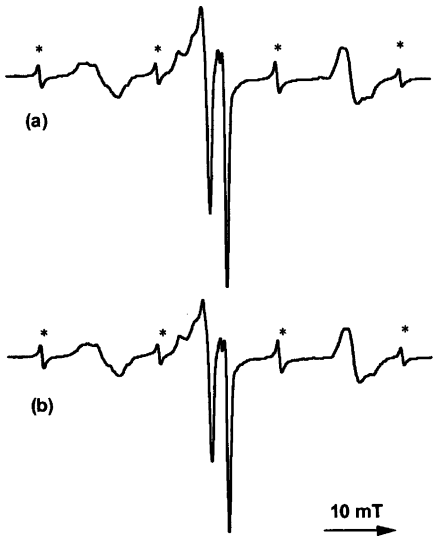

Figure 13. EPR spectra of MgO (a) after $^{13}CO_2$ adsorption under photoirradiation and (b) upon standing for 1 h in the dark. Asterisks indicate Mn^{2+} impurity in MgO.

the $CO_2 + CH_4$ reaction. On the other hand, it was confirmed by FT-IR spectroscopy that a surface formate was formed on MgO when acetaldehyde was introduced to MgO. We cannot assert whether the acetate species is active or not. In conclusion, we observed that the surface bidentate formate is a photoactive species for the CO_2 photocatalytic reduction and will discuss the role of the surface bidentate acetate in a future paper.

Conclusion

In the present study, we uncovered the mechanism of the CO_2 photocatalytic reduction in the presence of H_2 or CH_4 as a reductant. CO_2 adsorbed on MgO is activated to a CO_2^- radical under photoirradiation, and the CO_2^- radical was reduced to the surface bidentate formate in the presence of H_2 and CH_4 in the dark. It was identified that the photoactive species is the surface bidentate formate. This species, which was very stable on MgO, reduced CO_2 in the gas phase to CO under photoirradiation. In addition, it was clarified that the species was derived from the only side-on adsorption-type bidentate carbonate although the two bidentate carbonate were detected by FT-IR spectroscopy. It is isolated that the photocatalytic reaction proceeds over the stable species adsorbed on insulating materials such as MgO. This phenomenon is not explained by the conventional band theory, which is based on the excitation of electrons from the valence band to the conduction band of semiconductor material. We proposed the new concept to the band theory for the photocatalytic reaction.

References and Notes

(1) Inoue, T.; Fujishima, A.; Konishi, S.; Honda, K. *Nature* **1979**, *277*, 637.
(2) Hemminger, J. C.; Carr, R.; Somorjai, G. A. *Chem. Phys. Lett.* **1978**, *57*, 100.
(3) Fruge, D. R.; Fong, G. D.; Fong, F. K. *J. Am. Chem. Soc.* **1979**, *101*, 3694.
(4) Halmann, M. *Nature* **1978**, *275*, 115.
(5) Aurian-Blajeni, B.; Halmann, M.; Manassen, J. *Sol. Energy* **1980**, *25*, 165.
(6) Halmann, M.; Katzir, V.; Borgarello, E.; Kiwi, J. *Sol. Energy Mater.* **1984**, *10*, 85.
(7) Halmann, M.; Ulman, M.; Aurianblajeni, B. *Sol. Energy* **1983**, *31*, 429.
(8) Tennakone, K. *Sol. Energy Mater.* **1984**, *10*, 235.
(9) Tennakone, K.; Jayatissa, A. H.; Punchihewa, S. *J. Photochem. Photobiol. A: Chem.* **1989**, *49*, 369.
(10) Chandrasekaran, K.; Thomas, J. K. *Chem. Phys. Lett.* **1983**, *99*, 7.
(11) Anpo, M.; Chiba, K. *J. Mol. Catal.* **1992**, *74*, 207.
(12) Anpo, M.; Yamashita, H.; Ichihashi, Y.; Ehara, S. *J. Electroanal. Chem.* **1995**, *396*, 21.
(13) Anpo, M.; Yamashita, H.; Ikeue, K.; Fujii, Y.; Zhang, S. G.; Ichihashi, Y.; Park, D. R.; Suzuki, Y.; Koyano, K.; Tatsumi, T. *Catal. Today* **1998**, *44*, 327.
(14) Ikeue, K.; Yamashita, H.; Anpo, M.; Takewaki, T. *J. Phys. Chem. B* **2001**, *105*, 8350.
(15) Ikeue, K.; Nozaki, S.; Ogawa, M.; Anpo, M. *Catal. Lett.* **2002**, *80*, 111.
(16) Yamashita, H.; Kamada, N.; He, H.; Tanaka, K.; Ehara, S.; Anpo, M. *Chem. Lett.* **1994**, 855.
(17) Saladin, F.; Forss, L.; Kamber, I. *J. Chem. Soc., Chem. Commun.* **1995**, 533.
(18) Saladin, F.; Alxneit, I. *J. Chem. Soc., Faraday Trans.* **1997**, *93*, 4159.
(19) Ogura, K.; Kawano, M.; Yano, J.; Sakata, Y. *J. Photochem. Photobiol. A: Chem.* **1992**, *66*, 91.
(20) Thampi, K. R.; Kiwi, J.; Gratzel, M. *Nature* **1987**, *327*, 506.
(21) Kohno, Y.; Hayashi, H.; Takenaka, S.; Tanaka, T.; Funabiki, T.; Yoshida, S. *J. Photochem. Photobiol. A: Chem.* **1999**, *126*, 117.
(22) Kohno, Y.; Yamamoto, T.; Tanaka, T.; Funabiki, T. *J. Mol. Catal. A: Chem.* **2001**, *175*, 173.
(23) Aliwi, S. M.; Aljubori, K. F. *Sol. Energy Mater.* **1989**, *18*, 223.
(24) Kohno, Y.; Tanaka, T.; Funabiki, T.; Yoshida, S. *Chem. Commun.* **1997**, 841.
(25) Kohno, Y.; Tanaka, T.; Funabiki, T.; Yoshida, S. *Chem. Lett.* **1997**, 993.
(26) Kohno, Y.; Tanaka, T.; Funabiki, T.; Yoshida, S. *J. Chem. Soc., Faraday Trans.* **1998**, *94*, 1875.
(27) Kohno, Y.; Tanaka, T.; Funabiki, T.; Yoshida, S. *Phys. Chem. Chem. Phys.* **2000**, *2*, 2635.
(28) Kohno, Y.; Tanaka, T.; Funabiki, T.; Yoshida, S. *Phys. Chem. Chem. Phys.* **2000**, *2*, 5302.
(29) Kohno, Y.; Ishikawa, H.; Tanaka, T.; Funabiki, T.; Yoshida, S. *Phys. Chem. Chem. Phys.* **2001**, *3*, 1108.
(30) Raman, C. V. *Proc. Indian Acad. Sci.* **1947**, *26A*, 339.
(31) Raman, C. V. *Proc. Indian Acad. Sci.* **1961**, *54A*, 205.
(32) Hanna, R. *J. Am. Ceram. Soc.* **1965**, *48*, 376.
(33) Evans, J. V.; Ehateley, T. L. *Trans. Faraday Soc.* **1967**, *63*, 2769.
(34) Jung, H. S.; Lee, J. K.; Kim, J. Y.; Hong, K. S. *J. Colloid Interface Sci.* **2003**, *259*, 127.
(35) Davydov, A. A.; Rubene, N. A.; Budneva, A. A. *Kinet. Katal.* **1979**, *19*, 779.
(36) Fukuda, Y.; Tanabe, K. *Bull. Chem. Soc. Jpn.* **1973**, *46*, 1616.
(37) Tsuji, H.; Shishido, T.; Okamura, A.; Gao, Y. Z.; Hattori, H.; Kita, H. *J. Chem. Soc., Faraday Trans.* **1994**, *90*, 803.
(38) Yanagisawa, Y.; Takaoka, K.; Yamabe, S.; Ito, T. *J. Phys. Chem.* **1995**, *99*, 3704.
(39) He, M. Y.; Ekerdt, J. G. *J. Catal.* **1984**, *87*, 381.
(40) Busca, G.; Lamotte, J.; Lavalley, J. C.; Lorenzelli, V. *J. Am. Chem. Soc.* **1987**, *109*, 5197.
(41) Shido, T.; Asakura, K.; Iwasawa, Y. *J. Catal.* **1990**, *122*, 55.
(42) Feng, O. Y.; Kondo, J. N.; Maruya, K.; Domen, K. *J. Chem. Soc., Faraday Trans.* **1997**, *93*, 169.
(43) Martin, C.; Martin, I.; Rives, V. *J. Mol. Catal.* **1992**, *73*, 51.
(44) Wang, G. W.; Hattori, H. *J. Chem. Soc., Faraday Trans. 1* **1984**, *80*, 1039.
(45) Peng, X. D.; Barteau, M. A. *Langmuir* **1989**, *5*, 1051.
(46) Xu, C.; Koel, B. E. *J. Chem. Phys.* **1995**, *102*, 8158.
(47) Garcia, A. R.; da Silva, J. L.; Ilharco, L. M. *Surf. Sci.* **1998**, *415*, 183.
(48) Natal-Santiago, M. A.; Hill, J. M.; Dumesic, J. A. *J. Mol. Catal. A: Chem.* **1999**, *140*, 199.
(49) Khaleel, A.; Kapoor, P. N.; Klabunde, K. J. *Nanostruct. Mater.* **1999**, *11*, 459.
(50) Zecchina, A.; Lofthouse, M. G.; Stone, F. S. *Faraday Trans. 1* **1975**, *71*, 1476.
(51) Tench, A. J.; Pott, G. T. *Chem. Phys. Lett.* **1974**, *26*, 590.
(52) Coluccia, S.; Deane, A. M.; Tench, A. J. *J. Chem. Soc., Faraday Trans. 1* **1978**, *74*, 2913.
(53) Coluccia, S.; Tench, A. J.; L., S. R. *J. Chem. Soc., Faraday Trans. 1* **1979**, *75*, 1769.
(54) Coluccia, S.; Barton, A.; Tench, A. J. *J. Chem. Soc., Faraday Trans. 1* **1981**, *77*, 2203.
(55) Anpo, M.; Yamada, Y.; Kubokawa, Y.; Coluccia, S.; Zecchina, A.; Che, M. *J. Chem. Soc., Faraday Trans. 1* **1988**, *84*, 751.
(56) Willner, I.; Maidan, R.; Mandler, D.; Durr, H.; Dorr, G.; Zengerle, K. *J. Am. Chem. Soc.* **1987**, *109*, 6080.
(57) Fujiwara, H.; Hosokawa, H.; Murakoshi, K.; Wada, Y.; Yanagida, S.; Okada, T.; Kobayashi, H. *J. Phys. Chem. B* **1997**, *101*, 8270.
(58) Kaneco, S.; Shimizu, Y.; Ohta, K.; Mizuno, T. *J. Photochem. Photobiol. A: Chem.* **1998**, *115*, 223.
(59) Lunsford, J. H.; Jayne, J. P. *J. Phys. Chem.* **1965**, *69*, 2182.
(60) Serway, R. A.; Marshall, S. A. *J. Chem. Phys.* **1967**, *46*, 1949.
(61) Serway, R. A.; Marshall, S. A. *J. Chem. Phys.* **1968**, *47*, 868.
(62) Smart, R. S. C.; Slager, T. L.; Little, L. H.; Greenler, R. G. *J. Phys. Chem.* **1973**, *77*, 1019.
(63) Meriaudeau, P.; Vedrine, J. C.; Taarit, Y. B.; Naccache, C. **1975**, *71*, 736.
(64) Kai, A.; Miki, T. *Radiat. Phys. Chem.* **1992**, *40*, 469.
(65) Noethig-Laslo, V.; Brecevic, L. *J. Chem. Soc., Faraday Trans.* **1998**, *94*, 2005.
(66) Noethig-Laslo, V.; Brecevic, L. *Phys. Chem. Chem. Phys.* **1999**, *1*, 3697.
(67) Noethig-Laslo, V.; Brecevic, L. *Phys. Chem. Chem. Phys.* **2000**, *2*, 5328.